Journal of Biological Physics (2019) 45:317–334
https://doi.org/10.1007/s10867-019-09531-7

ORIGINAL PAPER

Influence of electromagnetic waves, with maxima in the green or red range, on the morphofunctional properties of multipotent stem cells

A. S. Chernov[1] · D. A. Reshetnikov[2] · G. K. Ristsov[3] · Yu A. Kovalitskaya[4] · A. M. Ermakov[5] · A. A. Manokhin[2] · A. V. Simakin[6] · R. G. Vasilov[1] · S. V. Gudkov[6,7]

Received: 8 February 2019 / Accepted: 27 August 2019 / Published online: 8 October 2019

Abstract
This paper examines the effect of electromagnetic waves, with maxima in the green or red regions of the spectrum, on the morphofunctional state of multipotent mesenchymal stromal cells. The illumination regimes used in our experiments did not lead to any substantial heating of the samples; the physical parameters of the lighting were carefully monitored. When the samples were illuminated with a green light, no significant photostimulatory effect was observed. Red light, on the other hand, had an evident photostimulatory effect. It is shown that photostimulation with a red light decreases the enzymatic activities of mitochondrial dehydrogenases and enhances the viability of cells, their proliferative activity, and their ability to form bone tissue. It is also established that red light stimulates cell proliferation, while not activating the genes that increase the risk of the subsequent malignant transformation of cells or their death. This paper discusses the possible role of hydrogen peroxide in the processes examined.

Keywords Photostimulation · Reprogramming of cages by means of physical methods · Visible light · An expression of genes · Hydrogen peroxide

1 Introduction

Visible light is a necessary condition for the existence of life on Earth. It is a natural source of energy for most photosynthetic organisms [1]. Moreover, many important processes in animals (phototaxis, phototropism, photoperiodism, circadian rhythms, vision, etc.) are light-dependent [2]. More than a century ago, practitioners began to use light in therapeutic medicine, and in 1903, the Danish physician and researcher

✉ A. S. Chernov
c.h.e.r.n.o.v@rambler.ru

Extended author information available on the last page of the article

Nils Finsen received the Nobel Prize in Physiology and Medicine "for the development of effective methods of phototherapy" [3]. Finsen found that spectral bands of sunlight differed in their therapeutic efficiency. At the beginning of his research, he tested and selected suitable absorption filters but then switched to artificial light sources (the Finsen lamp) [4]. Finsen's discovery stimulated research in the field and throughout the twentieth century, a lot of information about the effects of visible light on biological objects was accumulated. Currently, querying the PubMed system for "light therapy" yields more than 92,000 articles, with their number growing exponentially. At the initial stage of those photobiology studies, the phenomena of photobiomodulation were investigated using optical filters and monochromators [5]. The next major milestone in studying the effects of visible light on living organisms was the invention of lasers [6] and laser-based techniques [7–9]. The use of lasers designated the beginning of studies of the effects of low-intensity laser radiation on biological objects [10]. Nowadays, lasers are largely superseded by LED illuminators. Thus, a vast body of information has been accumulated over the past century, which is summarized in a huge number of works [11–20]. Currently, sources of visible light are used in practical medicine, especially in physiotherapy and photodynamic therapy, as well as for diagnostics of a number of diseases [21].

The effect of visible light on different organs, tissues and types of human cells is known to vary [13]. The most susceptible to this effect are dividing cells, which, under normal circumstances, are not exposed to electromagnetic radiation of a visible range [22]. Bone marrow cells are a type of dividing cell; they have been investigated extensively—in part, due to their potential use in replacement and rehabilitation therapy [23]. A large number of pathologies are known to be associated with bone marrow cells and the approaches based on the stimulation of bone marrow cells (including the photostimulation technique) have been studied for a long time [24–27]. In experiments with transplantation of bone marrow cells to rabbits [28] and rats [29], visible light was shown to have a significant photostimulatory effect. The treatment of skin wounds with donor bone marrow cells was also more effective when the treatment procedure included exposure to visible light [30, 31].

In most of the publications we analyzed, researchers used light sources with green and/or red emission, with the irradiance at the surface of the illuminated objects ranging from 0.1 to 30.0 W/m^2. There is much controversy in the data on the use of light sources with green or red emission. This is probably due to the fact that bone marrow contains various cellular fractions, which may have different primary targets for visible light. Moreover, cells of one of the bone marrow fractions may be affected by the intracellular signals transmitted by the cells of other fractions. It is not exactly clear how cells of the main bone marrow fraction—namely, multipotent mesenchymal stromal cells (MMSC)—are photostimulated under these conditions.

In this work, experiments were conducted on the culture of MMSC, with the cells being illuminated by light sources with green and red emission. The average irradiance at the surface of illuminated samples was about 1 W/m^2, which was in the range of the irradiance values used by other authors. The culture of primary human fetal fibroblasts (PHFF) was used as a control. The experiments showed that only red light had a significant effect on the morphofunctional state of MMSC. The effect of green light seemed to be secondary; it was probably mediated by the signals transmitted by the cells of another bone marrow fraction.

2 Materials and methods

2.1 Cell cultures

MMSC were allocated from the femur of male mice of the CD-1 line. The separation of multipotent mesenchymal stromal cells from blood cells and hematopoietic stem cells was carried out by means of the procedure described in [32]. The purified suspension of cells was cultivated in a CO_2-incubator at 37 °C and the maintenance of CO_2 in an atmosphere of 5%. We used the DMEM cultural media from a 10% solution of fetal bovine serum (Sigma, USA). The fibroblast of an integument of a human fetus (PHFF) used for comparison was allocated from the abortive material of a fetus. Cultivation of cells was carried out in DMEM/F-12 medium, from a 10% solution of fetal bovine serum, a L-glutamine (2 mm), penicillin (100 units/ml), and streptomycin (100 μg/ml) (Sigma, USA) at 37 °C in an atmosphere of 5% of CO_2.

2.2 Assessment of viability of cells

The assessment of viability of cells was carried out on a microscope Axiovert 200 (Carl Zeiss, Germany). In order to carry out the analysis, we used the Live/Dead Cell Viability Assays Kit (TermoFisher, USA), which provides a simple, two-color fluorescence assay that distinguishes metabolically active cells from injured cells and dead cells. The assay is based on the reduction of C12-resazurin to red-fluorescent C12-resorufin ($\lambda_{ex} = 488$ нм, $\lambda_{em} = 575$ нм) in metabolically active cells and on the uptake of the cell-impermeant, green-fluorescent nucleic acid stain, SYTOX Green dye ($\lambda_{ex} = 488$ нм, $\lambda_{em} = 530$ нм), in cells with compromised plasma membranes (usually late apoptotic and necrotic cells). Dyes were added onto the medium (5 mg/ml), and then the plate was located in a CO_2-incubator for 15 min; thereafter microphotographing of cells was carried out [33]. The surface occupied with cells was determined through different times after influence by the technique described earlier [34].

2.3 Assessment of differentiation potential

An assessment of the differentiation potential of mesenchymal stromal cells of mouse marrow investigated their ability of osteogene differentiation in response to particular differentiation incentives. For the induction of a differentiation of cell predecessors, they were cultivated in the environment with the addition of osteogene differentiation incentives (dexamethasone (10 nM), glitserol-2-phosphate (10 mM), and 2-phospho-L-acidum ascorbic (0.2 mM) (Sigma, USA)). Late stages of the osteogene differentiation of cells, estimated by coloring the calcinated matrix components with alizarin red (Prime Chemicals Group, Russia) with the addition of an oxyhydroxide of ammonium [35], obtained the quantitative data by means of processing of microphotographs in ImageJ.

2.4 Assessment of enzymatic activity of mitochondrial dehydrogenases

The assessment of enzymatic activity of mitochondrial dehydrogenases was carried out by a special water-soluble dye 3 (4,5-dimethylmetathiazole-2-ooze)-2.5-diphenyl-2H-tetrazolium bromide (Sigma, USA), whose dehydrogenases translate slightly soluble formazan. A measurement of dye was added to the medium of cultivation of cells at a concentration of 5 mg/ml. Within 5 min, the culture of cells was actively stirred up by means of a rocking chair and then

placed in a CO_2-incubator for 3 h. A transfer of formazan in the aqueous phase was made by an organic solvent of dimethyl sulfoxide (Fluka, Germany). The optical density of the received solutions was measured on Microplate Reader 680 XR (BioRad, France) at 540 nm. When calculating, we considered that 14.14 μg of formazan in 3 ml corresponded to one unit of optical density with a length of optical paths of 1 cm [36].

2.5 Measurement of concentration of hydrogen peroxide

The concentration of hydrogen peroxide was measured by the method of reinforced chemoluminescence in system luminol-4-iodinephenol-peroxidase. A luminometer used a highly sensitive lumenmeter of Biotoks 7 AM (Ekon, Russia). The experimental details of the method have been described earlier [37]. The high sensitivity of the method allows to record hydrogen peroxide in concentrations less than 1 nm [38]. The content of hydrogen peroxide was determined with the use of gauge schedules of dependence of a chemoluminescence on the known concentration of hydrogen peroxide in solution. The initial concentration of the hydrogen peroxide used for calibration was defined by a spectrophotometer at 240 nm with the use of coefficient of molar absorption 43.6 $M^{-1} \times cm^{-1}$ [39]. The initial concentration of hydrogen peroxide in the water was about 5 nM.

2.6 RT PCR

The definition of change of gene expression was carried out by the RT PCR method as described earlier [40]; information about the used primers is presented in Table 1. The PCR mode was as follows: (1) "hot start" (for an exception of not specific annealing of primers) at 95 °C, 5 min., (2) denaturation at 95 °C, 15 s, (3) annealing of primers and synthesis at 60 °C, 40 s. Stages 2–3 were repeated 40 times. The determination of values of a threshold cycle—Ct was carried out by means of the software BioRad (USA). The level of gene expression was normalized to that of the housekeeping genes cytoskeletal actin (Actb), ribosomal protein (RPLP), and glyceraldehyde 3-phosphate dehydrogenase (GADPH). The processing of results was carried out by a standard technique [41]. Changes of level of an expression of genes represented control values observed in intact cells.

2.7 Influence of visible light

In the experiments, we used two types of light-emitting diodes (Osram, Germany), with green and red emissions. The dispersion of light-emitting diodes on intensity did not exceed 5%; with a radiation divergence angle of approximately 40°. The definition of the spectral characteristics of the luminous fluxes was carried out by means of a USB3000T spectrometer (OceanOptics, USA) in the range 300 to 1000 nm. The definition of the power characteristics of luminous fluxes was carried out with the help of the automatic Field Master complex (Coherent, the USA) having a constant spectral response in the range 310 to 2800 nm. The characteristic ranges of the light-emitting diodes are presented in Fig. 1. It shows a working wavelength of the light-emitting diodes designated as green—525 nm and red—632 nm. A half-width of a spectrum line for the green light-emitting diode equaled 26 nm (512–538 nm) and for red 25 nm (625–640 nm). Apparently from a tab to the drawing 1 power density significantly depends on the working distance between the surface of diodes and objects. In order that the radiation

Table 1 Oligonucleotides used for qRT-PCR

Genes	GenBank accession #	Oligonucleotide 5′–3′
Alkaline phosphatase, liver/bone/kidney, ALPL	NM_000478.4	CATGCTGAGTGACACAGACAAGAA ACCGCCCACCACCTTGTAG
Bone gamma-carboxyglutamate protein, BGLAP	NM_199173.4	GGTGCAGAGTCCAGCAAAGG GCGCCTGGGTCTCTTCACTA
Bone morphogenetic protein 1, BMP1	NM_006129.4	AGGGCAATGATGTGTGCAAGT GCCATGCAGCTTGGAGTCA
bone morphogenetic protein receptor, type IA, BMPR1A	NM_004329.2	TCAGCGAACTATTGCCAAACAG TTGCCCATCCATACTTCTCCAT
Collagen, type I, alpha 1, COL1A1	NM_000088.3	CGATGGCTGCACGAGTCA CAGGCGGGAGGTCTTGGT
Collagen type III alpha 1, COL3A1	NM_000090.3	TGGAGGATGGTTGCACGAA GTAGTCTCACAGCCTTGCGTGTT
Epidermal growth factor receptor, EGFR	NM_005228.3	CTGAGCTCTCTGAGTGCAACCA CAGCTTTGCAGCCCATTTCT
Fibroblast growth factor 2, FGF-2	NM_002006.4	CGGTCAAGGAAATACACCAGTTG GCCCAGGTCCTGTTTTGGAT
Fibroblast growth factor receptor 1, FGFR1	NM_015850.3	TGCACCAACGAGCTGTACATG CTGCTTGAAGGTGGGTCTCTGT
Insulin-like growth factor 1, IGF1	NM_000618.3	TGCTTCCGGAGCTGTGATCT GCTGACTTGGCAGGCTTGAG
Insulin-like growth factor 1 receptor, IGFR1	NM_000875.3	ACGGCATGGCATACCTCAAC TTCGGCTACCATGCAATTCC
Runt-related transcription factor 2, RUNX2	NM_004348.3	GTATGTCCGCCACCACTCACTAC GAAGGGTCCACTCTGGCTTTG
Homolog 2, similar to mothers against decapentaplegic, SMAD2	NM_005901.5	GACACCAGTTTTGCCTCCAGTATT TCCAGAGGCGGAAGTTCTGTT
Homolog 4, similar to mothers against decapentaplegic, SMAD4	NM_005359.5	CATTGGATGGGAGGCTTCAG TCCAGAGACGGGCATAGATCA
Homolog 5, similar to mothers against decapentaplegic, SMAD5	NM_005903.6	AGGAACCTGAGCCACAATGAAC GTTGTTGGGCTGGTGGAAAG
Secreted phosphoprotein 1, SPP1	NM_000582.2	TTCGCAGACCTGACATCCAGTA CCATTCAACTCCTCGCTTTCC
Transforming growth factor beta receptor 1, TGFBR1	NM_004612.2	TGTGCTTCGTCTGCATCTCACT

Table 1 (continued)

Genes	GenBank accession #	Oligonucleotide 5′–3′
		TGGCACTCGATGGTGAATGA
Tumor necrosis factor, TNF	NM_000594.3	AGGCCAAGCCCTGGTATGA
		GCTGAGTCGGTCACCCTTCTC
Vitamin D receptor, VDR	NM_000376.2	GCTGGACGCCCACCATAA
		CTCCACCATCATTCACACGAACT
Cyclin-dependent kinase inhibitor 1B, CDKN1B	NM_004064.4	GCCAGCGCAAGTGGAATTT
		CTCCACCTCTTGCCACTCGTA
TNF receptor associated factor 2, TRAF2	NM_021138.3	GGCCGTCTGTCCCAGTGAT
		TTCGTGGCAGCTCTCGTATTC
Cluster differentiation 40 molecule, CD40	NM_001250.4	ACACTGCCACCAGCACAAATACT
		CTGTTTCTGAGGTGCCCTTCTG
Tumor necrosis factor receptor superfamily, member 1A, TNFRSF1	NM_003844.3	CTGGCGCTTGGGTCTCCTA
		TGCGTTGCTCAGAATCTCGTT
Aldehyde dehydrogenase 1 family member A1, ALDH1A1	NM_000689.4	GCAGTGAAGGCCGCAAGA
		CCCTCTCGGAAGCATCCATAG

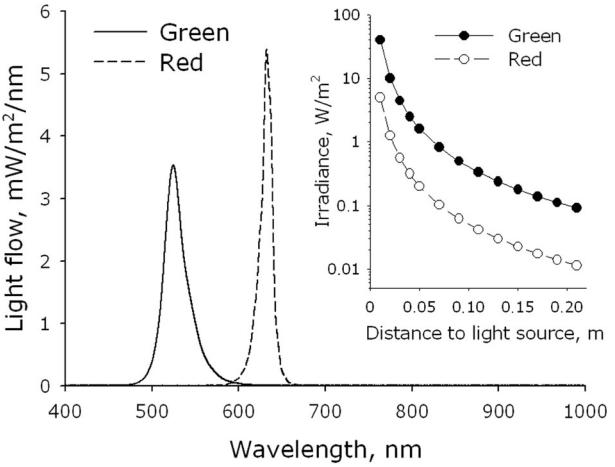

Fig. 1 Energy spectra of visible light sources (LED arrays). The energy spectrum of the matrix with emission in the green region of the spectrum (green) was measured from a distance of 3 cm, red (red)—1 cm. The inset shows the dependence of energy efficiency on the working distance between the surface of the diodes and the object

power density on a surface of exemplars influenced by green and red light-emitting diodes was equal, the distance from an object to light-emitting diodes was 7 and 2 cm respectively. The radiation power density on a surface of exemplars under such circumstances was about 1.2 W/m^2. Cages were irradiated in cultural strip tablets (8 × 12 small cavities). During the radiation, the strip tablet was sorted and divided into three groups (control, green, red), 4 columns in each (8 × 4 wells). Radiation by electromagnetic waves, with maxima in green or red spectral ranges, was carried out in the conditions of a CO_2 incubator. During the radiation, the medium was replaced with DMEM fenol red free (Sigma, USA). Control specimens were not exposed to light; however, replacement of the environment in them was made. To prevent evaporation of the culture medium during irradiation, the plates were covered with an optically transparent plastic. In order to prevent the exposure of light to neighboring wells, the bottom and walls of all wells were covered with a light-tight polymeric material.

3 Results

In the preliminary experiments, we investigated the effect of green and red light on the intensity of energy metabolism, which was judged by the activity of mitochondrial dehydrogenases. The irradiation regimes varied by the duration of light exposure (7.5, 15, 30, and 60 min), corresponding to the final irradiation doses of 540, 1080, 2160, and 4320 J/m^2 respectively. The 7.5-min and 15-min exposures were shown to be not long enough for the appearance of any substantial changes in the activity of mitochondrial dehydrogenases. Increasing the time of exposure to 30 min resulted in the development of evident biological effects. When the exposure time was further increased to 60 min, the manifestation of the beneficial effects was significantly reduced. Since the photomodulatory effect was maximal at the exposure time of 30 min, this regime was used in all the subsequent experiments. It should be noted that the effects registered in those experiments were quite stable: they developed within 4 h after irradiation and persisted for several days.

Figure 2 shows changes in the activity of mitochondrial dehydrogenases caused by the irradiation of MMSC and PHFF cultures for 3 days with green or red light. One can see that in both cultures, the activity of mitochondrial dehydrogenases decreased. The response of MMSC and PHFF to irradiation was quite similar, yet the inhibitory effect of green light was less pronounced comparatively to the effect of red light (up to 15 and 30% inhibition respectively).

Figure 3 shows evaluation of viability of MMSC and PHFF after a 3-day exposure to green or red light. It was found that the green light did not change viability of cells of both types. At the same time, exposure of MMSC and PHFF to red light resulted in the development of substantial effects. The number of viable cells in the MMSC culture increased by a factor of 1.4 after the exposure, whereas the number of dead cells decreased by ~40%. In the PHFF culture, the number of viable cells increased by a factor of 1.2, and the number of dead cells—although not changing much—still showed a tendency to decrease (by ~10%).

The effect of green and red light on the ability of MMSC and PHFF to colonize the surface of culture substrates is shown in Fig. 4. It should be noted that the cells did not always form a monolayer, sometimes multilayer formations and cell aggregates were observed. The dynamics of the process had a sigmoidal character, with the rate of cell division and colonization being the highest in the period of 3rd–9th day. After the 11th day, no differences between the experimental groups were observed. The median of culture colonization (the time taken by the cells to occupy 50% of the culture substrate) was about 5 days for MMSC and 6 days for PHFF.

The experiments showed that green light did not affect the rate of cell division; the values of colonization median were the same as in the control samples (5 days for MMSC and 6 days for PHFF). Exposure of the cultures to red light, on the other hand, resulted in a substantial increase in the rate of cell division and culture colonization. In the samples irradiated with red light, the values of colonization median were about 4 days for MMSC and 5.5 days for PHFF. In terms of the relative rate of substrate colonization, the area colonized by MMSC in the samples irradiated with red light was 20% larger by the 5th day comparatively with the control samples. For PHFF, the area gain under these conditions amounted to 15%.

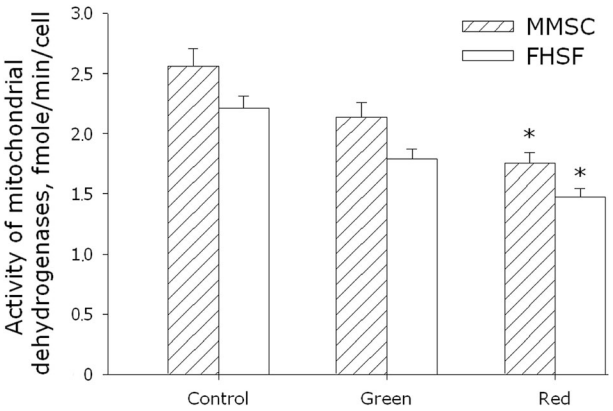

Fig. 2 Evaluation of enzymatic activity of mitochondrial dehydrogenases of MMSC and PHFF lines on the 3rd day after exposure to electromagnetic waves with maxima in the green or red regions of the spectrum. Data are represented as the means ± SEM of three independent experiments. The asterisks mark the values that significantly differ from the control at $p < 0.05$ (Student's unpaired t test)

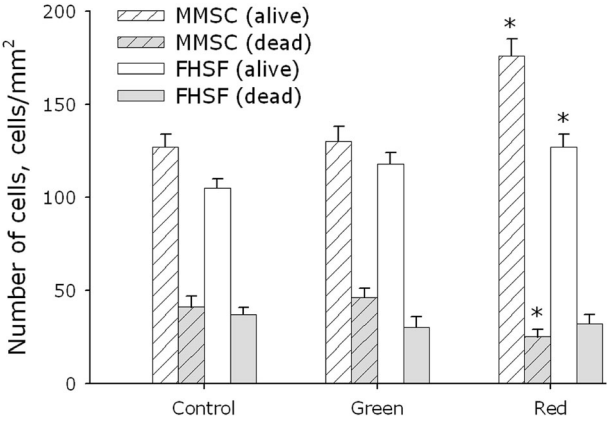

Fig. 3 Evaluation of cell viability of MMSC and PHFF lines on the 3rd day of cultivation after exposure to electromagnetic waves with maxima in the green or red regions of the spectrum. Data are represented as the means ± SEM of four independent experiments. The asterisks mark the values that significantly differ from the control at $p < 0.05$ (Student's unpaired t test)

In this work, we also investigated the effect of green and red light on the rate of formation of crystalline calcium phosphate in the culture of MMSC. For the initiation of calcium phosphate crystallization in the MMSC culture, an osteogenic inductive mixture was used. Its application led to the emergence of evident signs of differentiation, formation of a crystalline structure of calcium phosphate. The effect of green and red light on the rate of calcium phosphate crystallization in the MMSC culture is shown in Fig. 5. As one can see on the control samples, the formation of calcium deposits linearly depended on the cultivation time. When the cells were exposed to green light, the rate of accumulation of calcium deposits, which was monitored for 19 days, did not differ from that in the control samples. Irradiation with red light, however, caused a sharp acceleration of deposit accumulation. By the 5th day of the experiment, the samples irradiated with red light showed a 2.9-fold increase, as compared with the control, in the amount of accumulated calcium deposits. By the 11th day, the amount of deposits was 2.3-fold of that in the control samples, and by the 19th day, the value declined to a 1.4-fold difference.

To understand what molecular mechanisms underlie the effects of green and red light, we analyzed the level of expression of a number of genes. The main focus of the analysis was on the genes of the so-called fetal proteins, osteogenic factors, and cell cycle regulators. Changes in the expression level of a gene allow judging of the likelihood of manifestation of the gene-encoded trait, since the content of the corresponding mRNA often correlates with the probability of development of the trait. Table 2 shows the dynamics of relative changes in the gene expression levels, which were observed in the culture of PHFF irradiated with green or red light.

In the analysis of gene expression, we considered the difference between the experiment and control samples to be significant when the expression level changed by a factor of 5. The analysis showed that the number of genes whose expression level changed was much lower when PHFF were irradiated with green light—comparatively with the situation when the cells were exposed to red light. A 2-h exposure of PHFF to green light led to a drop in the levels of gene expression of

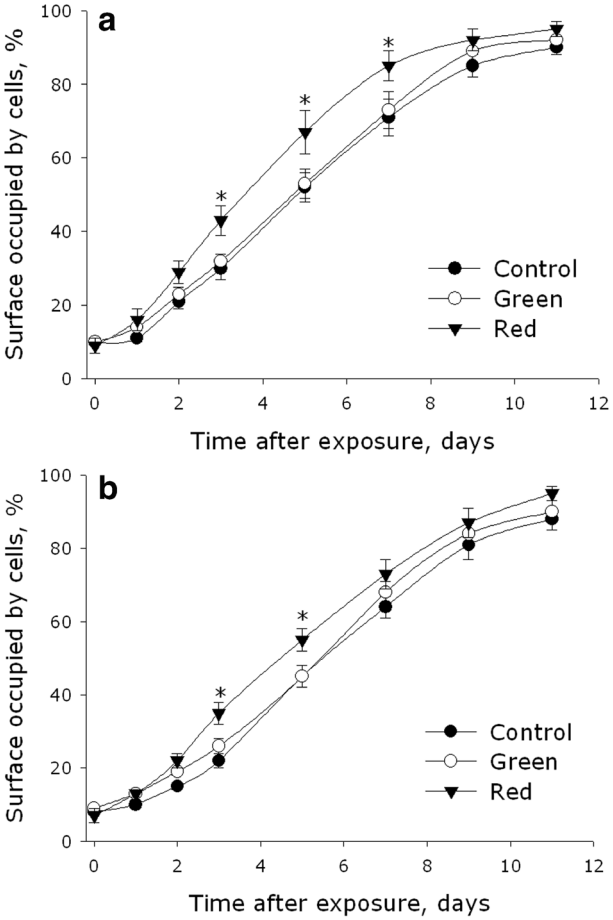

Fig. 4 Effect of electromagnetic waves with maxima in the green or red regions of the spectrum on the ability of MMSC (**a**) and PHFF (**b**) cell cultures to colonize the surface of culture substrates. Data are represented as the means ± SEM of four independent experiments. The asterisks mark the values that significantly differ from the control at $p < 0.05$ (Student's unpaired t test)

osteogenic differentiation markers (IGF1 and BGLAP) and a rise in the levels of gene expression of the regulatory cytokine TNF and the dehydrogenase ALDH1A1, which regulates a major switch between metabolic pathways. Irradiation of samples with red light resulted in a similar response and, additionally, altered the expression of a number of other genes. Specifically, there was an increase in the levels of gene expression of ALPL and IGF1R, as well as SPP1, which is responsible for bone mineralization. There was also a drop in the levels of gene expression of some other proteins; transcription factor RUNX2; receptor VDR, which affects mineral exchange; and marker CD40. A 1-day exposure of PHFF samples to visible light (both green and red) led to the growth of the levels of gene expression of BGLAP, ALDH1A1, SPP1, VDR, and proapoptotic factor CDKN1B. Red light additionally caused changes in the levels of gene expression of ALPL, CD40, and TRAF2. After 2 days of irradiation, the profile of gene expression changed—yet, in general, the response of

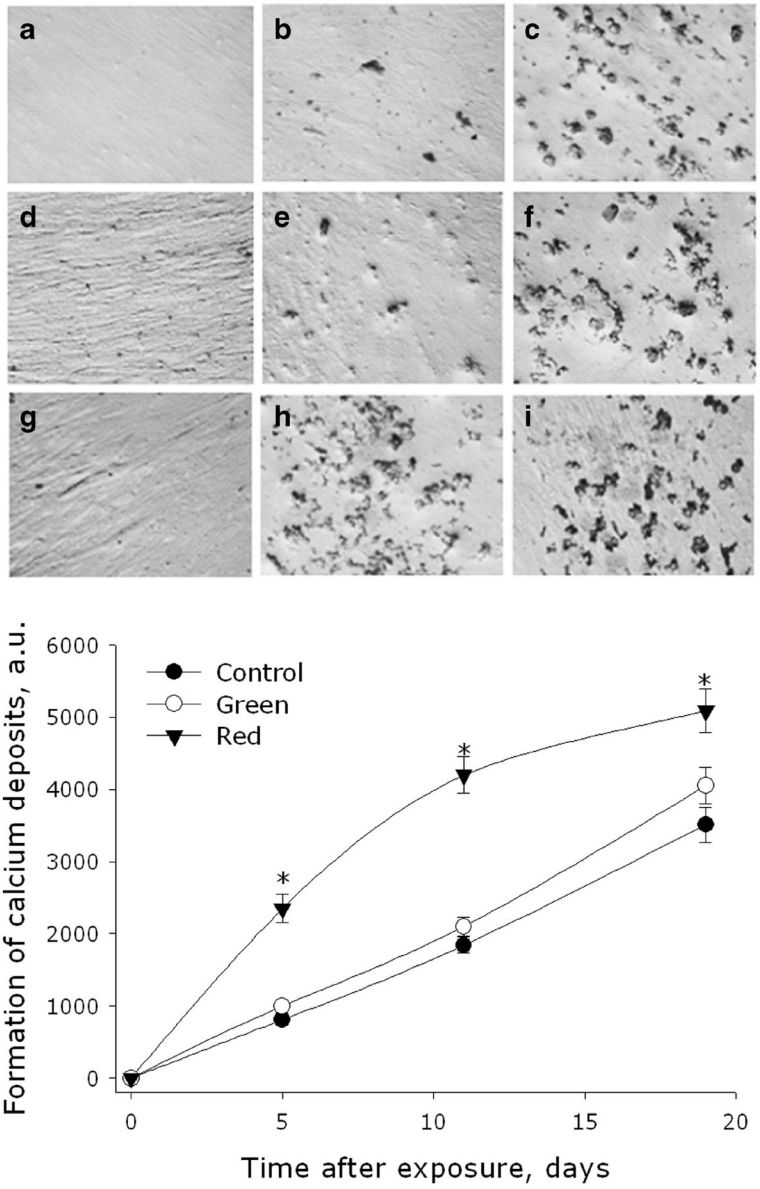

Fig. 5 Effect of electromagnetic waves, with maxima in the green or red regions of the spectrum, on the formation rate of crystalline calcium phosphate in MMSC culture. Representative micrographs are presented. Micrographs show colored crystalline calcium phosphate in intact cells (**a**–**c**) and cells exposed to green (**d**–**f**) and red (**j**–**i**) light. The cells were cultured for 5 (**a**, **d**, **f**), 11 (**b**, **e**, **h**), and 19 (**c**, **f**, **i**) days. The graph shows the numerical values characterizing the calcification of cells. Data are represented as the means ± SEM of three independent experiments. The asterisks mark the values that significantly differ from the control at $p < 0.05$ (Student's unpaired *t* test)

genes of different groups to the stimulus persisted, with the expression of genes of the TNF superfamily changing by two orders of magnitude in a number of cases.

Table 2 Relative changes in the levels of gene expression in MMSC culture at different times after exposure to electromagnetic waves with maxima in the green or red regions of the spectrum

Genes	Relative levels of gene expressions					
	After 2 h		After 1 day		After 2 day	
	Green	Red	Green	Red	Green	Red
ALPL	−1.4	7.1*	1.4	−132.5*	3.4	5.3*
BGLAP	−9.1*	−22.5*	16.1*	12.5*	−1.2	−2.1
BMP1	−1.1	−1.3	3.6	1.2	2.7	3.5
BMPR1A	1.3	1.4	1.74	1.0	1.6	10.4
COL1A1	1.0	−1.2	2.8	1.8	1.3	2.4
COL3A1	−1.0	−1.3	1.3	1.8	1.6	3.1
EGFR	1.8	1.0	2.9	2.6	1.1	2.5
FGF-2	−1.2	−2.2	1.8	2.1	2.1	2.0
FGFR1	1.4	1.3	1.6	1.5	−1.7	−1.1
IGF1	−7.0*	−5.1*	−3.2	−1.0	4.1	1.1
IGFR1	−1.1	7.4*	1.9	−2.1	−1.4	2.0
RUNX2	1.6	−12.8*	4.7	2.8	−1.6	−1.4
SMAD2	−1.0	1057	2.6	2.3	1.2	19.2*
SMAD4	−2.6	−4112	2.5	1.8	1.9	11.1*
SMAD5	1.40	1.8	1.6	1.5	−1.4	3.7
SPP1	−1.0	30.3*	15.7*	74.0*	5.7*	7.0*
TGFBR1	−1.5	1.0	1.6	−2.3	2.8	2.7
TNF	21.8*	23.5*	−3.8	−1.8	−1.1	−481.0*
VDR	1.7	−6.4*	6.7*	6.0*	−17.5*	10.0*
CDKN1B	−1.1	2.0	101.1*	179.7*	203.6*	49.8*
TRAF2	2.0	−3.0	1.79	−65.7*	34.0*	101.8*
CD40	1.3	−8.5*	−1.0	−202.2*	−1.3	−21.7*
TNFRSF1	−1.9	28.284	−2.8	1.5	1.0	−377.4*
ALDH1A1	270.6*	205.0*	31.7*	89.2*	−4.7	−14.7*

*The difference between the expression level and control values is more than 5 times

The experiment was repeated 5 times. In some cases, the obtained data did not satisfy the hypothesis of a normal distribution, therefore, non-parametric statistics were used for comparative analysis. Relative changes in gene expression levels were calculated using the formula $N = N_{exp}/N_{cont}$, where N_{exp} is the distribution median obtained by the action of red or green light, and N_{cont} is the distribution median obtained in control experiments.

The analysis described above revealed changes in the expression of a number of redox-sensitive genes, and correspondingly, an assumption was made that irradiation with visible light led to the formation of reactive oxygen species (ROS). The most stable ROS is known to be H_2O_2; its concentration can be measured in native aqueous solutions, not containing any dyes or other chemicals—after the exposure to visible light is finished. We wanted to measure the maximal possible yield of H_2O_2 under the effect of visible light, so we conducted control experiments in which we deliberately avoided the use of any complex colloidal systems, imitating the cellular content. The formation of H_2O_2 in water under irradiation with green and red light is shown in Fig. 6. In control samples (not exposed to light), no substantial changes in the concentration of H_2O_2 were observed. Exposure of samples to green or red light resulted in the formation of H_2O_2, whose concentration grew linearly with the time of exposure. The rate of H_2O_2 formation was 0.2 nM/min (~ 3 pM ×

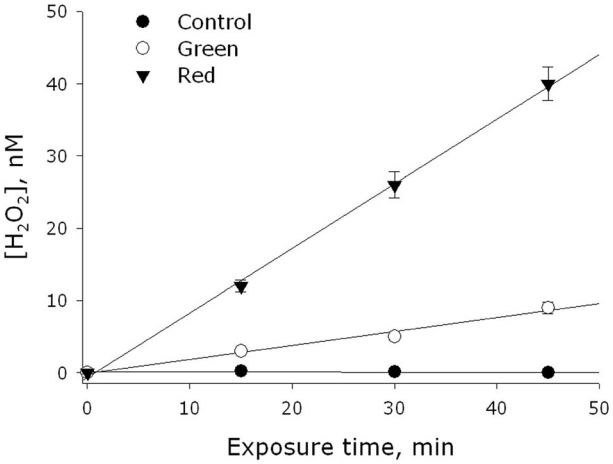

Fig. 6 Generation of hydrogen peroxide in water under the action of electromagnetic waves with maxima in the green or red regions of the spectrum. The background level of H_2O_2 was subtracted from the observed values

m^2/J) in the case of green light and about 0.9 nM/min (~ 12.5 pM × m^2/J) in the case of red light. Thus, the amount of H_2O_2 formed under irradiation with red light was about 4.5-fold of the amount formed under the effect of green light.

4 Discussion

The experiments with cell cultures showed that green light had no substantial photostimulatory effect on MMSC (Figs. 2, 3, 4, 5). Irradiation of the cells with red light, on the other hand, resulted in photostimulation (Figs. 2, 3, 4, 5). Comparison of the two cultures, MMSC and PHFF, revealed that MMSC were more responsive to photostimulation (Figs. 2, 3, 4, 5). A key result was demonstration of the possibility to stimulate the processes of cell division and development (Figs. 3, 4). Mitogenic stimuli, enhancing cell division, often lead to the formation of cancer cells [42]. In our experiments, we did not find any changes in the expression of genes associated with the malignant transformation of cells—despite the fact of an accelerated proliferation of cells, preceding their redirection to the osteogenic pathway of development (Table 1). This fact allows us to suppose that, in contrast to the methods used earlier, the procedure of photostimulation suggested in the paper would not increase susceptibility of cells to malignization [43–46]. It should be noted that some reports describe a phenomenon of enhanced respiratory activity of cells and a related increase in cell tumorogenity [46]. In our experiments, on the other hand, a decrease in the activity of mitochondrial dehydrogenases was observed, which suggests a lowered respiratory activity of cells (Fig. 2). The causes of changes in the respiratory activity of cells are not known. Changes can be associated directly with the activity of enzymes or general changes in mitochondria [47]. This may be a compensatory effect associated with mitochondrial degradation [48]. On the other hand, this may be an effect associated with a change in the concentration of the free calcium cation or the activation of certain signaling and regulatory pathways of metabolism [49].

Irradiation of MMSC with red light was also found to cause intensive osteogenesis, a faster differentiation of MMSC into the cells of bone tissue (Fig. 5). Earlier, researchers from South Korea developed a technology of dentin regeneration using photostimulation with red light [50]. Red light activated dental stem cells, promoting transition of the TFG-beta factor into the active form. TFG-beta is present in mammal cells mainly in the latent form and is activated by ROS, which are generated under the effect of visible light [50].

It should be noted that ROS are involved in the modulation of a large number of regulatory systems of the cell and the organism [51]. Of all the ROS, the main secondary messenger in the organism of mammals is H_2O_2 [52]. It is constantly generated in living cells—both as a result of normal metabolism and under the effect of external factors (ionizing, ultraviolet, EHF, and microwave radiation; vibration; heat; visible; and infrared radiation in the range of absorption lines of molecular oxygen) [53–57]. Living organisms contain a large number of systems, utilizing H_2O_2 and stabilizing its concentration [58]. As shown above, irradiation of aqueous solutions with the light sources used in our experiments leads to the formation of H_2O_2 (Fig. 6). Earlier it was established that dipoles of oxygen molecules dissolved in water are photoreceptors of laser radiation (632.8 and 1264 nm), which is based on their transition into the singlet state [59]. This phenomenon is called the light-oxygen effect. The general scheme of H_2O_2 formation with the light-oxygen effect was established earlier [60]. Of course, the concentration of ROS can change not only as a result of their direct formation. Not less important is the indirect effect of light on the concentration of ROS, which is described in the literature [61, 62].

5 Conclusion

The results of this work show that irradiation of multipotent mesenchymal stromal cells with red light can cause their photostimulation. Green light, in contrast, does not have a significant photostimulatory effect on the cells. The irradiation regimes used in our experiments do not lead to any substantial changes in the temperature of the samples. Irradiation of cells with red light is shown to decrease the enzymatic activity of mitochondrial dehydrogenases and enhance viability and proliferative activity of the cells. The stimulation of multipotent mesenchymal stromal cells with red light leads to more intensive osteogenesis and the development of bone tissue. The analysis of gene expression suggests that red light can stimulate proliferation of cells without the risk of their subsequent malignant transformation. The results obtained also indirectly indicate that H_2O_2 can play a certain role in the processes of photostimulation.

Funding information The optical part of the work was carried out with the support of R&D program (0024-2019-0004).

Compliance with ethical standards

Conflict of interest The authors declare that they have no conflict of interest.

References

1. Gudkov, S.V., Andreev, S.N., Barmina, E.V., Bunkin, N.F., Kartabaeva, B.B., Nesvat, A.P., Stepanov, E.V., Taranda, N.I., Khramov, R.N., Glinushkin, A.P.: Effect of visible light on biological objects: physiological

and pathophysiological aspects. Phys. Wave Phenom. **25**, 207 (2017). https://doi.org/10.3103/S1541308X17030074
2. Gehring, W.J.: The evolution of vision. Wiley Interdiscip. Rev. Dev. Biol. **3**(1), 1 (2014). https://doi.org/10.1002/wdev.96
3. Lectures, N.: Physiology or medicine 1901–1921. Elsevier Publ, Amsterdam (1967)
4. Bie, V.: Remarks on Finsen's phototherapy. Br. Med. J. **2022**, 825 (1899)
5. Barnard, J.E., Morgan, H.R.: The physical factors in phototherapy. Br. Med. J. **2**(2237), 1269 (1903)
6. Tew Jr., J.M., Tobler, W.D.: The laser: history, biophysics, and neurosurgical applications. Clin. Neurosurg. **31**, 506 (1983)
7. Sarimov, R.M., Matveyeva, T.A., Binhi, V.N.: Laser interferometry of the hydrolytic changes in protein solutions: the refractive index and hydration shells. J. Biol. Phys. **44**(3), 345 (2018). https://doi.org/10.1007/s10867-018-9494-7
8. Chung, W.J., Cui, Y., Chen, C.S., Wei, W.H., Chang, R.S., Shu, W.Y., Hsu, I.C.: Freezing shortens the lifetime of DNA molecules under tension. J. Biol. Phys. **43**(4), 511 (2017). https://doi.org/10.1007/s10867-017-9466-3
9. Trnka, J., Nedomová, Š., Kumbár, V., Šustr, M., Buchar, J.: A new approach to analyze the dynamic strength of eggs. J. Biol. Phys. **42**(4), 525 (2016). https://doi.org/10.1007/s10867-016-9420-9
10. Karu, T.: Photobiology of low-power laser effects. Health Phys. **56**, 691 (1989)
11. Chung, H., Dai, T., Sharma, S.K., Huang, Y., Carroll, J.D., Hamblin, M.R.: The nuts and bolts of low-level laser (light) therapy. Ann. Biomed. Eng. **40**, 516 (2012). https://doi.org/10.1007/s10439-011-0454-7
12. Passarella, S., Karu, T.: Absorption of monochromatic and narrow band radiation in the visible and near IR by both mitochondrial and non-mitochondrial photoacceptors results in photobiomodulation. J. Photochem. Photobiol. B **140**, 344 (2014). https://doi.org/10.1016/j.jphotobiol.2014.07.021
13. Monich, V.A., Bavrina, A.P., Malinovskaya, S.L.: Modification in oxidative processes in muscle tissues exposed to laser- and light-emitting diode radiation. Lasers Med. Sci. **33**(1), 159 (2018). https://doi.org/10.1007/s10103-017-2370-z
14. Deryugina, A.V., Ivashchenko, M.N., Ignatiev, P.S., Balalaeva, I.V., Samodelkin, A.G.: Low-level laser therapy as a modifier of erythrocytes morphokinetic parameters in hyperadrenalinemia. Lasers Med. Sci. (2019). https://doi.org/10.1007/s10103-019-02755-y
15. Nahhas, A.F., Mohammad, T.F., Hamzavi, I.H.: Vitiligo surgery: shuffling melanocytes. J. Investig. Dermatol. Symp. Proc. **18**(2), S34 (2017). https://doi.org/10.1016/j.jisp.2017.01.001
16. Caldieraro, M.A., Cassano, P.: Transcranial and systemic photobiomodulation for major depressive disorder: a systematic review of efficacy, tolerability and biological mechanisms. J. Affect. Disord. **243**, 262 (2018). https://doi.org/10.1016/j.jad.2018.09.048
17. Korkina, L.G.: Current trends in medicinal chemistry of photoprotection and phototherapy. Curr. Med. Chem. **25**(40), 5466 (2018). https://doi.org/10.2174/0929867325401811201046 20
18. Santana-Blank, L., Rodríguez-Santana, E., Santana-Rodríguez, K.E., Reyes, H.: "Quantum leap" in photobiomodulation therapy ushers in a new generation of light-based treatments for cancer and other complex diseases: perspective and mini-review. Photomed. Laser Surg. **34**(3), 93 (2016). https://doi.org/10.1089/pho.2015.4015
19. Lapchenko, A.S., Kucherov, A.G., Order, R.Y., Lapchenko, A.A.: Antimicrobial anti-inflammatory photodynamic and light-emitting-diode phototherapy of the consequences of the gunshot and mine-blast injury to the face, head, and neck including damage to the ENT organs. Vestn. Otorinolaringol. **83**(1), 62 (2018). https://doi.org/10.17116/otorino201883162-64
20. Comorosan, S., Kappel, W., Constantinescu, I., Gheorghe, M., Ionescu, E., Pîrvu, C., Cinca, S., Cristache, L.: Green light effects on biological systems: a new biophysical phenomenon. J. Biol. Phys. **35**(3), 265 (2009). https://doi.org/10.1007/s10867-009-9164-x
21. Reddy, G.K.: Photobiological basis and clinical role of low-intensity lasers in biology and medicine. J. Clin. Laser Med. Surg. **22**, 141 (2004). https://doi.org/10.1089/104454704774076208
22. Chernov, A.S., Reshetnikov, D.A., Kovalitskaya, Y.A., Manokhin, A.A., Gudkov, S.V.: Influence of wideband visible light with an padding red component on the functional state of mice embryos and embryonic stem cells. J. Photochem. Photobiol. B **188**, 77 (2018). https://doi.org/10.1016/j.jphotobiol.2018.09.007
23. Paim, Á., Tessaro, I.C., Cardozo, N.S.M., Pranke, P.: Mesenchymal stem cell cultivation in electrospun scaffolds: mechanistic modeling for tissue engineering. J. Biol. Phys. **44**(3), 245 (2018). https://doi.org/10.1007/s10867-018-9482-y
24. Emel'yanov, A.N., Kir'yanova, V.V.: The application of stem cells together with visible and infrared light in regenerative medicine (part 2). Vopr. Kurortol. Physiother. Lecheb. Physiol. Cult. **92**, 43 (2015). https://doi.org/10.17116/kurort2015243-51

25. Tuby, H., Maltz, L., Oron, U.: Induction of autologous mesenchymal stem cells in the bone marrow by low-level laser therapy has profound beneficial effects on the infarcted rat heart. Laser. Surg. Med. **43**, 401 (2011). https://doi.org/10.1002/lsm.21063
26. Pyczek, M., Sopala, M., Dabrowski, Z.: Effect of low-energy laser power on the bone marrow of the rat. Folia Biologica (Krakow). **42**, 151 (1994)
27. Zhang, H., Hou, J.F., Shen, Y., Wang, W., Wei, Y.J., Hu, S.: Low level laser irradiation precondition to create friendly milieu of infarcted myocardium and enhance early survival of transplanted bone marrow cells. J. Cell. Mol. Med. **14**, 1975 (2010). https://doi.org/10.1111/j.1582-4934.2009.00886.x
28. Nagata, M.J., Santinoni, C.S., Pola, N.M., De Campos, N., Messora, M.R., Bomfim, S.R., Ervolino, E., Fucini, S.E., Faleiros, P.L., Garcia, V.G., Bosco, A.F.: Bone marrow aspirate combined with low-level laser therapy: a new therapeutic approach to enhance bone healing. J. Photochem. Photobiol. B **121**, 6 (2013). https://doi.org/10.1016/j.jphotobiol.2013.01.013
29. Shefer, G., Ben-Dov, N., Halevy, O., Oron, U.: Primary myogenic cells see the light: improved survival of transplanted myogenic cells following low energy laser irradiation. Laser. Surg. Med. **40**, 38 (2008). https://doi.org/10.1002/lsm.20588
30. Choi, K., Kang, B.J., Kim, H., Lee, S., Bae, S., Kweon, O.-K., Kim, W.H.: Low-level laser therapy promotes the osteogenic potential of adipose-derived mesenchymal stem cells seeded on an acellular dermal matrix. J. Biomed. Mater. Res. B. **101B**, 919 (2013). https://doi.org/10.1002/jbm.b.32897
31. Yang, C.C., Wang, J., Chen, S.C., Hsieh, Y.L.: Synergistic effects of low-level laser and mesenchymal stem cells on functional recovery in rats with crushed sciatic nerves. J. Tissue Eng. Regenerat. Med. **10**, 120 (2013). https://doi.org/10.1002/term.1714
32. Nardi, N.B., Camassola, M.: Isolation and culture of rodent bone marrow-derived multipotent mesenchymal stromal cells. Methods Mol. Biol. **698**, 151 (2011). https://doi.org/10.1007/978-1-60761-999-4_12
33. Johnson, M.B., Criss, A.K.: Fluorescence microscopy methods for determining the viability of bacteria in association with mammalian cells. J. Vis. Exp. **79**, 50729 (2013). https://doi.org/10.3791/50729
34. Sevost'yanov, M.A., Nasakina, E.O., Baikin, A.S., Sergienko, K.V., Konushkin, S.V., Kaplan, M.A., Seregin, A.V., Leonov, A.V., Kozlov, V.A., Shkirin, A.V., Bunkin, N.F., Kolmakov, A.G., Simakov, S.V., Gudkov, S.V.: Biocompatibility of new materials based on nano-structured nitinol with titanium and tantalum composite surface layers: experimental analysis in vitro and in vivo. J. Mater. Sci. Mater. Med. **29**, 33 (2018). https://doi.org/10.1007/s10856-018-6039-3
35. Meirelles, L.S., Nardi, N.B.: Murine marrow-derived mesenchymal stem cell: isolation, in vitro expansion, and characterization. Br. J. Haematol. **123**, 702 (2003). https://doi.org/10.1046/j.1365-2141.2003.04669.x
36. Stossel, T.P.: Evaluation of opsonic and leukocyte function with a spectrophotometric test in patients with infection and with phagocytic disorders. Blood **42**, 121 (1973)
37. Bruskov, V.I., Popova, N.R., Ivanov, V.E., Karp, O.E., Chernikov, A.V., Gudkov, S.V.: Formation of long-lived reactive species of blood serum proteins by the action of heat. Biochem. Biophys. Res. Commun. **443**, 957 (2014). https://doi.org/10.1016/j.bbrc.2013.12.073
38. Chernikov, A.V., Gudkov, S.V., Shtarkman, I.N., Bruskov, V.I.: Oxygen effect in heat-mediated damage to DNA. Biofizika **52**(2), 244 (2007). https://doi.org/10.1134/S0006350907020078
39. Gudkov, S.V., Guryev, E.L., Gapeyev, A.B., Sharapov, M.G., Bunkin, N.F., Shkirin, A.V., Zabelina, T.S., Glinushkin, A.P., Sevost'yanov, M.A., Belosludtsev, K.N., Chernikov, A.V., Bruskov, V.I., Zvyagin, A.V.: Unmodified hydrated C(60) fullerene molecules exhibit antioxidant properties, prevent damage to DNA and proteins induced by reactive oxygen species and protect mice against injuries caused by radiation-induced oxidative stress. Nanomedicine **15**(1), 37 (2019). https://doi.org/10.1016/j.nano.2018.09.001
40. Ermakov, A.M., Chernov, A.S., Selezneva, I.I., Poltavtseva, R.A.: A study of the impacts of low-intensity light irradiation in the red (λ_{max} = 635 nm) and green (λ_{max} = 520 nm) ranges on the proliferative activity and gene expression profiles of MNNG/hos cells and human fetal fibroblasts. Biofizika **62**, 63 (2017). https://doi.org/10.1134/S0006350917010055
41. Sharapov, M.G., Novoselov, V.I., Fesenko, E.E., Bruskov, V.I., Gudkov, S.V.: The role of peroxiredoxin 6 in neutralization of X-ray mediated oxidative stress: effects on gene expression, preservation of radiosensitive tissues and postradiation survival of animals. Free Radic. Res. **51**, 148 (2017). https://doi.org/10.1080/10715762.2017.1289377
42. Liao, D.J., Thakur, A., Wu, J., Biliran, H., Sarkar, F.H.: Perspectives on c-Myc, cyclin D1, and their interaction in cancer formation, progression, and response to chemotherapy. Crit. Rev. Oncog. **13**, 93 (2007). https://doi.org/10.1615/CritRevOncog.v13.i2.10
43. Eweida, A., Rosenbauer, O., Frisch, O., Giordano, F.A., Fleckenstein, J., Wenz, F., Kirschner, S., Brockmann, M.A., Schulte, M., Kneser, U., Harhaus, L.: Irradiation delays tissue growth but enhances osteogenic differentiation in vascularized constructs. J. Reconstr. Microsurg. (2018). https://doi.org/10.1055/s-0038-1667048

44. Wang, L., Zhang, J., Wang, C., Qi, Y., Du, M., Liu, W., Yang, C., Yang, P.: Low concentrations of TNF-α promote osteogenic differentiation via activation of the ephrinB2-EphB4 signalling pathway. Cell Prolif. **50**(1), e12311 (2017). https://doi.org/10.1111/cpr.12311
45. Zhou, F., Huang, H., Zhang, L.: Bisindoylmaleimide I enhances osteogenic differentiation. Protein Cell **3**(4), 311 (2012). https://doi.org/10.1007/s13238-012-2027-4
46. Selezneva, I.I., Savintseva, I.V., Vikhlyantseva, E.F., Davydova, G.A., Gavrilyuk, B.K.: Immobilization and long-term culturing of mouse embryonic stem cells in collagen-chitosan gel matrix. Bull. Exp. Biol. Med. **142**(1), 119 (2006). https://doi.org/10.1007/s10517-006-0308-8
47. Denton, R.M.: Regulation of mitochondrial dehydrogenases by calcium ions. Biochim. Biophys. Acta **1787**(11), 1309 (2009). https://doi.org/10.1016/j.bbabio.2009.01.005
48. Belosludtsev, K.N., Belosludtseva, N.V., Tenkov, K.S., Penkov, N.V., Agafonov, A.V., Pavlik, L.L., Yashin, V.A., Samartsev, V.N., Dubinin, M.V.: Study of the mechanism of permeabilization of lecithin liposomes and rat liver mitochondria by the antimicrobial drug triclosan. Biochim. Biophys. Acta Biomembr. **1860**(2), 264 (2018). https://doi.org/10.1016/j.bbamem.2017.09.018
49. Belosludtsev, K.N., Dubinin, M.V., Belosludtseva, N.V., Mironova, G.D.: Mitochondrial Ca^{2+} transport: mechanisms, molecular structures, and role in cells. Biochemistry (Mosc.) **84**(6), 593 (2019). https://doi.org/10.1134/S0006297919060026
50. Park, J.S., Park, K.H.: Light enhanced bone regeneration in an athymic nude mouse implanted with mesenchymal stem cells embedded in PLGA microspheres. Biomater. Res. **20**, 4 (2016). https://doi.org/10.1186/s40824-016-0051-9
51. Vaahtera, L., Brosché, M., Wrzaczek, M., Kangasjärvi, J.: Specificity in ROS signaling and transcript signatures. Antioxid. Redox Signal. **21**, 1422 (2014). https://doi.org/10.1089/ars.2013.5662
52. Tamma, G., Valenti, G., Grossini, E., Donnini, S., Marino, A., Marinelli, R.A., Calamita, G.: Aquaporin membrane channels in oxidative stress, cell signaling, and aging: recent advances and research trends. Oxidative Med. Cell. Longev. **2018**, 1501847 (2018). https://doi.org/10.1155/2018/1501847
53. Ward, J.F.: DNA damage produced by ionizing radiation in mammalian cells: identities, mechanisms of formation and reparability. Progr. Nucl. Acid Res. Mol. Biol. **35**, 95 (1988)
54. Gapeyev, A.B., Lukyanova, N.A., Gudkov, S.V.: Hydrogen peroxide induced by modulated electromagnetic radiation protects the cells from DNA damage. Cent. Eur. J. Biol. **9**, 915 (2014). https://doi.org/10.2478/s11535-014-0326-x
55. Vandamme, M., Robert, E., Lerondel, S., Sarron, V., Ries, D., Dozias, S., Sobilo, J., Gosset, D., Kieda, C., Legrain, B., Pouvesle, J.M., Pape, A.L.: ROS implication in a new antitumor strategy based on non-thermal plasma. Int. J. Cancer **130**, 2185 (2012). https://doi.org/10.1002/ijc.26252
56. Gudkov, S.V., Lyakhov, G.A., Pustovoy, V.I., Shcherbakov, I.A.: Influence of mechanical effects on the hydrogen peroxide concentration in aqueous solutions. Phys. Wave Phenom. **27**(2), 141 (2019). https://doi.org/10.3103/S1541308X19020092
57. Piskarev, I.M.: Hydrogen peroxide formation in aqueous solutions under UV-C radiation. High Energ. Chem. **52**, 212 (2018). https://doi.org/10.1134/S0018143918030128
58. Sharapov, M.G., Goncharov, R.G., Gordeeva, A.E., Novoselov, V.I., Antonova, O.A., Tikhaze, A.K., Lankin, V.Z.: Enzymatic antioxidant system of endotheliocytes. Dokl. Biochem. Biophys. **471**(1), 410 (2016). https://doi.org/10.1134/S1607672916060090
59. Zakharov, S.D., Ivanov, A.V.: Light-oxygen effect in cells and its potential applications in tumour therapy (review). Quantum Electron. **29**, 1031 (1999). https://doi.org/10.1070/QE1999v029n12ABEH001629
60. Gudkov, S.V., Karp, O.E., Garmash, S.A., Ivanov, V.E., Chernikov, A.V., Manokhin, A.A., Astashev, M.E., Iaguzhinskii, L.S., Bruskov, V.I.: Generation of reactive oxygen species in water under exposure of visible or infrared irradiation at absorption band of molecular oxygen. Biofizika **57**(1), 5 (2012). https://doi.org/10.1134/S0006350912010113
61. George, S., Hamblin, M.R., Abrahamse, H.: Effect of red light and near infrared laser on the generation of reactive oxygen species in primary dermal fibroblasts. J. Photochem. Photobiol. B **188**, 60 (2018). https://doi.org/10.1016/j.jphotobiol.2018.09.004
62. Sun, Q., Kim, H.-E., Cho, H., Shi, S., Kim, B., Kim, O.: Red light-emitting diode irradiation regulates oxidative stress and inflammation through SPHK1/NF-κB activation in human keratinocytes. J. Photochem. Photobiol. B **186**, 31 (2018). https://doi.org/10.1016/j.jphotobiol.2018.05.015

Affiliations

A. S. Chernov[1] · D. A. Reshetnikov[2] · G. K. Ristsov[3] · Yu A. Kovalitskaya[4] · A. M. Ermakov[5] · A. A. Manokhin[2] · A. V. Simakin[6] · R. G. Vasilov[1] · S. V. Gudkov[6,7]

[1] National Research Center "Kurchatov Institute", Akademika Kurchatova pl. 1, Moscow, Russia 123182

[2] Institute of Cell Biophysics, Federal Research Center "Pushchino Scientific Center for Biological Research of the Russian Academy of Sciences", Russian Academy of Sciences, Nauki Ave., 3, Pushchino, Moscow Region, Russia 142290

[3] Institute of Biochemistry and Physiology of Microorganisms, Federal Research Center "Pushchino Scientific Center for Biological Research of the Russian Academy of Sciences", Russian Academy of Sciences, Nauki Ave., 3, Pushchino, Moscow Region, Russia 142290

[4] Branch of the Shemyakin-Ovchinnikov Institute of Bioorganic Chemistry, Russian Academy of Sciences, Institutskaya St. 6, Pushchino, Moscow Oblast, Russia 142290

[5] Institute of Theoretical and Experimental Biophysics of the Russian Academy of Sciences, Institutskaya St. 6, Pushchino, Moscow Region, Russia 142290

[6] Prokhorov General Physics Institute of the Russian Academy of Sciences, Vavilova Ave., 38, Moscow, Russia 119991

[7] All-Russia Research Institute for Phytopathology, B. Vyazyomy, Moscow Region, Russia 143050